Lattice Boltzmann Method for Turbulent Heat Transfer in Wavy Channel Flows

H.Y. Lai, S. C. Chang, and W. L. Chen

Abstract—The hydrodynamic and thermal lattice Boltzmann methods are applied to investigate the turbulent convective heat transfer in the wavy channel flows. In this study, the turbulent phenomena are modeling by large-eddy simulations with the Smagorinsky model. As a benchmark, the laminar and turbulent backward-facing step flows are simulated first. The results give good agreement with other numerical and experimental data. For wavy channel flows, the distribution of Nusselt number and the skin-friction coefficients are calculated to evaluate the heat transfer effect and the drag force. It indicates that the vortices at the trough would affect the magnitude of drag and weaken the heat convection effects on the wavy surface. In turbulent cases, if the amplitude of the wavy boundary is large enough, the secondary vortices would be generated at troughs and contribute to the heat convection. Finally, the effects of different Re on the turbulent transport phenomena are discussed.

Keywords—Heat transfer, lattice Boltzmann method, turbulence, wavy channel.

I. INTRODUCTION

THE lattice Boltzmann equation (LBE) is developed from the lattice gas cellular automata (LGCA) by introducing ensemble-average density distribution function to substitute the Boolean operators in LGCA [1]. In the lattice Boltzmann method (LBM), the fluid flow is treated on a statistical level and calculated by a simplified kinetic model, in which macroscopic physical properties are associated with microscopic processes. This bottom-up scheme is different from traditional top-down schemes of computational fluid dynamics (CFD), which analyze flow fields by solving macroscopic variables in the Navier-Stokes equations. In recent years, the LBM has become a promising method of CFD, especially in mesoscopic engineering and science as microfluidics [2]. The LBM has been extensively applied to multiphase fluid flows [3], heat transfer [4], fluid flows through porous media [5], and etc. It possesses an advantage to implement boundaries with complex flow or fractal geometry [6].

Similar to LGCA, LBM performs a two-step evolution of particle distribution functions on a specific lattice model, namely particle distribution "collisions" on lattice nodes and

H. Y. Lai and S. C. Chang are with the Department of Mechanical Engineering, National Cheng Kung University, Tainan 701, Taiwan (e-mail: hylai@mail.ncku.edu.tw, mr_scchang@yahoo.com.tw).

W. L. Chen is a master's degree graduated student of the Department of Mechanical Engineering, National Cheng Kung University, Tainan 701, Taiwan (e-mail: cool-walin@hotmail.com).

stream "propagations" from one node to all neighbors along the lattice directions. After streaming, new local properties on lattice nodes are obtained by distribution components from neighbors, so that macroscopic properties of fluid flows can be calculated by solving this velocity discrete Boltzmann equation. In LBE, the complex collision terms of the Boltzmann equation can be replaced by a simplified relaxation model, namely the well-known Bhatnagar-Gross-Krook (BGK) model [7]. By the Chapman-Enskog expansion, this lattice BGK model can be recovered to the Navier-Stokes equations for hydrodynamics or to energy equation for heat transfer.

Simulating turbulent flows by the LBM is an attractive topic [8], [9]. The common methods for simulating turbulence are direct numerical simulation (DNS), Reynolds average numerical simulation (RANS), and large-eddy simulation (LES) [10]. The main idea of the LES is to decompose the turbulence into two parts of different scales, namely a large scale part solved by the Navier-Stokes equations and a small scale part described by a sub-grid scale (SGS) model. The LES has been used to solve many turbulent problems, e.g. simple hydraulic channels [10], gas turbine combustor flow [11], buoyant jets [12], free surface [13], and heat transfer for turbulent flows [14]. The SGS model used in this study is based on the well-known Smagorinsky model including vortex-viscous and vortex-diffusive forms [15]. Hou et al. [16] used LBM coupled with the standard Smagorinsky model to simulate two-dimensional driven cavity flow at Re up to 100,000. By solving the vorticity-stream function equations with the LES and Smagorinsky model, Chen [17] presented a lattice Boltzmann algorithm to simulate turbulent driven cavity flow. The numerical stability of this model is better than the traditional LBM, which solves mass density, pressure, and velocity for Navier-Stokes equations and has constraints of low Mach number and relaxation time. Guan et al. [18] introduced the dynamics SGS model and the dynamical system SGS model for the LBM to solve three dimensional high Re turbulent driven cavity flows. Results were compared with those obtained by the Smagorinsky model.

This paper adopts the hydrodynamic and thermal LBM algorithms to study the transport phenomena of the wavy channel, which is often employed to enhance the heat transfer efficiency in industrial processes [19]. Wang and Chen [20] used a simple coordinate transformation for the complex wavy boundary and solve the stream function, vorticity and energy equations of the fluid flow by the spline alternating-direction implicit method. The effects of the wavy geometry, Reynolds number (Re), and Prandtl number (Pr) on the skin-friction and

World Academy of Science, Engineering and Technology
International Journal of Aerospace and Mechanical Engineering
Vol:7, No:7, 2013

Nusselt number (Nu) were discussed. By the finite element method, Alawadhi [21] studied the steady fluid flow and heat transfer in a wavy channel of 25< Re<1000 with a linearly increasing waviness at the entrance region.

Since turbulent flows are common in nature and engineering, the present study focuses on the turbulent transport phenomena of fluid flow in wavy channels. The LES method is adopted for the LBM simulation of turbulence. As a benchmark, the laminar and turbulent backward-facing step flows are simulated first to validate the feasibility of this LBM-LES method for an open flow system. The result of the reattachment length is compared with other experimental and simulation data [22]–[25]. For wavy channels, the effects of wavy geometry, Reynolds number and Prandtl number on hydrodynamic and heat transfer phenomena are discussed simultaneously. The magnitude of drag and heat transfer efficiency are evaluated by inspecting the skin-friction coefficient ($\mathrm{Re}\,C_f$) and the Nusselt number on the wavy surface.

II. NUMERICAL METHODS

A. Lattice Boltzmann Hydrodynamic Model

In the LBM simulation of incompressible flows, the continuity equation and Navier-Stokes equations are solved by calculating the evolution of density distribution function according to the LBE on the lattice model. The Boltzmann equation with the BGK model can be written as follows:

$$\frac{\partial f}{\partial t} + \vec{v} \cdot \frac{\partial f}{\partial \vec{x}} = \frac{1}{\tau_f}\left(f^{eq} - f\right) \tag{1}$$

where $\vec{v}$ is microscopic velocity, and τ_f is the relaxation time for the density distribution function, f, towards the local equilibrium. The equilibrium distribution function f^{eq} is related to the Maxwell-Boltzmann equilibrium distribution. By applying a lattice model of a discrete velocity set, (1) is transformed into the discrete LBGK form and discretized in the time and space domain as

$$f_\alpha\left(\vec{x} + \vec{e}_\alpha \Delta t, t + \Delta t\right) - f_\alpha\left(\vec{x}, t\right)$$
$$= -\frac{1}{\tau_f}\left[f_\alpha\left(\vec{x}, t\right) - f_\alpha^{eq}\left(\vec{x}, t\right)\right] \tag{2}$$

where $f_\alpha\left(\vec{x}, t\right)$ and $\vec{e}_\alpha$ are the component of density distribution function and lattice velocity vector in α direction of the lattice model. Equation (2) represents that in each time step, the stream and collision steps are performed individually at nodes with different lattice directions Therefore, this algorithm is suitable for parallel computation.

In the LBM simulation, the common lattice model is the DnQb model [26], which refers to the number n of dimensional sublattices and to the discrete number b of spatial translation lattice vectors. This present work adopts the D2Q9 lattice model

[6] for both the hydrodynamic and thermal analysis of flows. The discrete velocity set of D2Q9 model in Fig. 1 is defined as

$$\begin{cases} \vec{e}_0 = \left(0, 0\right) \\ \vec{e}_{1,3}, \vec{e}_{2,4} = \left(\pm c, 0\right), \left(0, \pm c\right) \\ \vec{e}_{5,6,7,8} = \left(\pm c, \pm c\right) \end{cases} \tag{3}$$

where $c = \Delta x/\Delta t = \Delta y/\Delta t$ is the lattice streaming speed related to the run time step, Δt, and the grid spacing Δx and Δy. The density equilibrium distribution function is given by

$$f_\alpha^{eq} = \rho \omega_\alpha \left[1 + \frac{\vec{e}_\alpha \cdot \vec{u}}{c_s^2} + \frac{\left(\vec{e}_\alpha \cdot \vec{u}\right)^2}{2c_s^4} - \frac{u^2}{2c_s^2}\right] \tag{4}$$

where $\vec{u}\left(\vec{x}, t\right)$ is the velocity vector at the lattice node of position $\vec{x}$. The weight parameters are $\omega_0 = 4/9$, $\omega_{1,2,3,4} = 1/9$, and $\omega_{5,6,7,8} = 1/36$ respectively. The local density and velocity are obtained by

$$\rho = \sum_\alpha f_\alpha \tag{5}$$

$$\vec{u} = \frac{1}{\rho}\sum_\alpha f_\alpha \vec{e}_\alpha \tag{6}$$
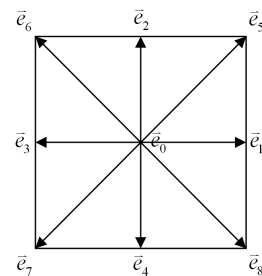

Fig. 1 D2Q9 model for LBM simulation

By the Chapman-Enskog expansion, this LBGK model can be recovered to the governing equations of incompressible flow at low Mach number with the pressure, $p = \rho c_s^2$, related to the lattice sound speed, $c_s = c/\sqrt{3}$. The kinematic viscosity is given by $\nu = c_s^2\left(\tau_f - 0.5\right)\Delta t$.

B. Lattice Boltzmann Thermal Model

Similar to the hydrodynamic model, the macroscopic energy equation can be derived from a LBM algorithm for the temperature distribution function by Chapman-Enskog expansion. The thermal LBM model used in this paper is proposed by Shan [27], which is based on the model for simulating flows with multi-phases and -components [28]. In this model, the heat transfer of fluid flow is calculated by the evolution equation of temperature distribution function, $g_\alpha\left(\vec{x}, t\right)$, as

World Academy of Science, Engineering and Technology
International Journal of Aerospace and Mechanical Engineering
Vol:7, No:7, 2013

$$g_\alpha\left(\bar{x}+\bar{e}_\alpha\Delta t,t+\Delta t\right)-g_\alpha\left(\bar{x},t\right)$$
$$=-\frac{1}{\tau_g}\left[g_\alpha\left(\bar{x},t\right)-g_\alpha^{eq}\left(\bar{x},t\right)\right] \qquad (7)$$

where τ_g is the relaxation time. The temperature equilibrium distribution function for the D2Q9 lattice model is given by

$$g_\alpha^{eq}=T\omega_\alpha\left[1+\frac{\bar{e}_\alpha\cdot\bar{u}}{c_s^2}+\frac{\left(\bar{e}_\alpha\cdot\bar{u}\right)^2}{2c_s^4}-\frac{u^2}{2c_s^2}\right] \qquad (8)$$

The local macroscopic temperature is calculated as

$$T=\sum_\alpha g_\alpha \qquad (9)$$

The diffusivity is $\kappa=c_s^2\left(\tau_g-0.5\right)\Delta t$.

C. LBM-LES Method

In the large-eddy simulation, the physical quantity Φ is decomposed into large and small scale parts by the filtering process as follows [10]

$$\bar{\Phi}=\frac{1}{\Delta^3}\cdot\int_{-\Delta/2}^{\Delta/2}\int_{-\Delta/2}^{\Delta/2}\int_{-\Delta/2}^{\Delta/2}\Phi(\bar{\xi},t)G(\bar{x}-\bar{\xi})d\xi_1 d\xi_2 d\xi_3 \qquad (10)$$

where Φ is the large scale physical quantity after filter process, and Δ is the filter length equal to the mesh length. The spatial filter function, G, is the box filter function as follows,

$$G\left(\bar{x}-\bar{\xi}\right)=\begin{cases}1 & ,\left|\bar{x}-\bar{\xi}\right|\le 0.5\Delta \\ 0 & ,\left|\bar{x}-\bar{\xi}\right|> 0.5\Delta\end{cases} \qquad (11)$$

By filtering the density and temperature distribution function, the hydrodynamic and thermal LBM-LES models with the same forms as before filtering can be obtained [16].

In the LBM-LES model, the viscosity are replaced by the equivalent quantity, $v_{total}=v+v_t$. By applying the Smagorinsky model, the eddy viscosity, v_t, is represented as

$$v_t=\left(C_s\Delta\right)^2\left|\bar{S}\right| \qquad (12)$$

where C_s is the Smagorinsky constant of a positive value. In this paper, the Smagorinsky constant is fixed as $C_s=0.1$. The magnitude of strain rate tensor $\left|\bar{S}\right|$ is calculated by

$$\left|\bar{S}\right|=\frac{\sqrt{\tau_f^2+\frac{18\sqrt{2}\left(C_s\Delta\right)^2 Q^{\frac{1}{2}}}{\rho}}-\tau_f}{6\left(C_s\Delta\right)^2} \qquad (13)$$

where Q represents the magnitude of the non-equilibrium stress tensor, Π_{ij}, and is calculated as

$$Q=\Pi_{ij}\Pi_{ij} \qquad (14)$$
$$\Pi_{ij}=\sum_\alpha e_{\alpha i}e_{\alpha j}\left(f_\alpha-f_\alpha^{eq}\right) \qquad (15)$$

Similarly, the equivalent diffusivity, $\kappa_{total}=\kappa+\kappa_t$, is used for the thermal LBM-LES model with introducing the eddy diffusivity, κ_t. For a fluid flow of specific Reynolds number, $\mathrm{Re}=UL/v$, and Prandtl Number, $\mathrm{Pr}=v/\kappa$, v and κ can be calculated according to the characteristic velocity and length of the flow field. The eddy diffusivity is also obtained by defining the sub-grid Prandtl Number as $\mathrm{Pr}_t=v_t/\kappa_t$.

D. Boundary Conditions and Convergence Criteria

In the LBM simulation, the boundary conditions are implemented by calculating the unknown components of distribution function on boundary nodes after streaming process. These unknowns are due to no propagation from the boundary into the flow and can be solved by applying appropriate method. In this study, the no-slip boundary condition of the stationary wall is realized by the unknown-index algorithm [6] and the common bounce-back rule [29]. The boundary condition of a given velocity or temperature is implemented by the forced-equilibrium method [16] as

$$f_\alpha\left(\bar{x}_b,t+\Delta t\right)=f_\alpha^{eq}\left(\bar{x}_b,t\right) \qquad (16)$$
$$g_\alpha\left(\bar{x}_b,t+\Delta t\right)=g_\alpha^{eq}\left(\bar{x}_b,t\right) \qquad (17)$$

where $\bar{x}_b$ represents the position at the boundary node.

For laminar flows, the criteria of convergence are as follows,

$$\frac{\sum_{i,j}\left|\vec{V}\left(\bar{x}_{i,j},t+\Delta t\right)-\vec{V}\left(\bar{x}_{i,j},t\right)\right|}{\sum_{i,j}\left|\vec{V}\left(\bar{x}_{i,j},t\right)\right|}\le 1.0\times 10^{-7} \qquad (18)$$

$$\frac{\sum_{i,j}\left|T\left(\bar{x}_{i,j},t+\Delta t\right)-T\left(\bar{x}_{i,j},t\right)\right|}{\sum_{i,j}\left|T\left(\bar{x}_{i,j},t\right)\right|}\le 1.0\times 10^{-7} \qquad (19)$$

In the turbulence, the unsteady flow phenomena are captured by evaluating the time average of physical quantities.

III. RESULTS AND DISCUSSION

In the LBM-LES simulation, all equations and physical quantity are non-dimensionalized by the lattice length, lattice speed, and reference density, ρ_0. The dimensionless temperature is defined as $T^*=(T-T_{in})/(T_w-T_{in})$. The numerical simulation is confirmed to be grid independent.

World Academy of Science, Engineering and Technology
International Journal of Aerospace and Mechanical Engineering
Vol:7, No:7, 2013

A. Benchmark

Fig. 2 is the schematic view of the backward-facing step flow. The expansion ratio and the Reynolds number are defined as $ER = H/h = 2$ and $\mathrm{Re} = U_{in}H/\nu$ with the average velocity of the fully-developed inlet flow, $U_{in} = 0.1c$. This inlet flow with a constant temperature at $T = T_{in}$ is placed at a distance of

$40h$ from the step. At the outlet of $L_{out} = 100h$, the flow with a fixed reference pressure is assumed to be fully developed, i.e. $\partial U/\partial x = \partial V/\partial x = \partial T/\partial x = 0$. All stationary walls adopt no-slip boundary conditions and a high constant temperature $T = T_w > T_{in}$. The Prandtl number and subgrid Prandtl Number are fixed to 1.0 and 0.7.
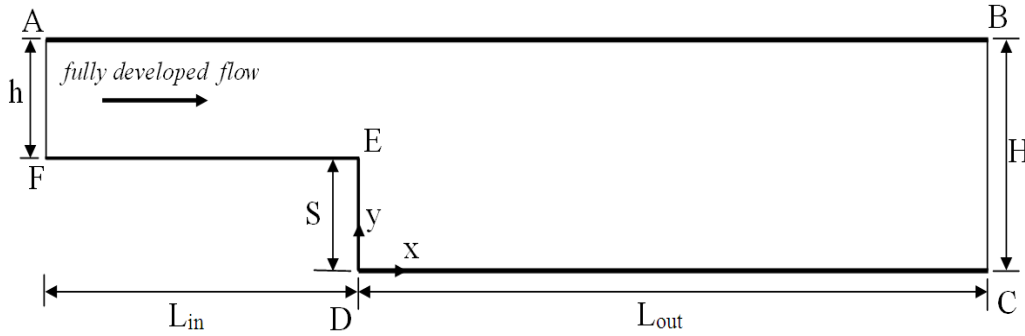
Fig. 2 Schematic view of the backward-facing step flow

In the backward-facing step flow, the separation and reattachment phenomena produce the recirculation region downstream the step. As Re increases, the main recirculation region downstream the step is enlarged accompanying with a secondary recirculation region produced near the upper wall. Fig. 3 shows the reattachment length of main recirculation region in laminar flows. The present results are close to other numerical and experiment results [22]–[24]. In turbulent backward-facing step flows, more small transient vortices behind the step are formed. The secondary vortex near upper wall is also smaller than that of laminar flow. Armaly et al. [22] indicated the main reattachment length almost kept constant at Re≧ 6,600. The results by LBM-LES model is listed in Table I with comparison to Armaly et al. [22] and Jongebloed's work [25].

Fig. 3 Reattachment points of laminar backward-facing step flow at different Re

TABLE I
REATTACHMENT LENGTHS FOR TURBULENT BACKWARD-FACING STEP FLOWS

Re	Armaly *et al.* [22]	Jongebloed [25]	Present results
6600	8.05909	-	8.84
7000	8.01919	6.92	8.68
8000	8.0211	6.80	8.1
9000	-	-	7.8

In the thermal field, the cold fluid from inlet is heating by the hot walls via the heat transfer between walls and fluid, and hence the fluid temperature is increased downstream, as shown in Figs. 4 and 5 for laminar and turbulent flows respectively. In laminar cases, an intermediate region of cold fluid is formed and expanded as Re increases. The thermal diffusivity is dominant near the wall boundary and in the region of recirculation. In turbulent cases, the flow field is strongly perturbed, and therefore the convective effect is dominant everywhere including wall boundaries and recirculation regions. The temperature distribution of fluid downstream is uniform with no intermediate region found, i.e. the fluid heating, or namely the wall cooling, is very fast and efficient in turbulence.

B. Transport Phenomena in Wavy Channel Flows

Fig. 6 shows the schematic view of the wavy channel flow in this study. The shape of the upper wavy-wall profile is given as

$$S(x) = L + a \sin\left[\pi(x - L_{in})/L\right] \qquad (20)$$

The amplitude-wavelength ratio α is defined as $\alpha = a/L$, and the Reynolds number is defined as $\mathrm{Re} = U_{in}L/\nu$. As in the backward-facing step flows, the cold fluid of $T = T_{in}$ flows through hot wavy surfaces of $T = T_w > T_{in}$ and turns into a fully developed flow at the outlet with a fixed reference pressure. The flat walls are also given a high temperature at T_w in turbulent

World Academy of Science, Engineering and Technology
International Journal of Aerospace and Mechanical Engineering
Vol:7, No:7, 2013

cases, but considered to be adiabatic in laminar cases for comparison with Wang and Chen's results [20]. In addition, all flat and wavy boundaries are no-slip.
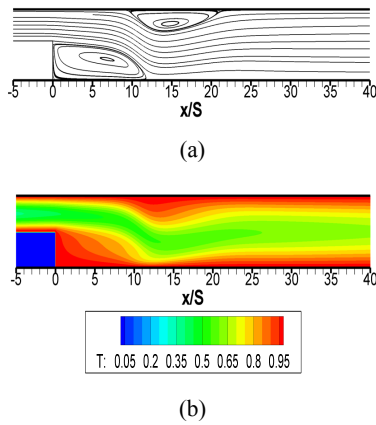

(a)

(b)

Fig. 4 (a) Streamlines and (b) temperature distribution of backward-facing step flows at Re=900
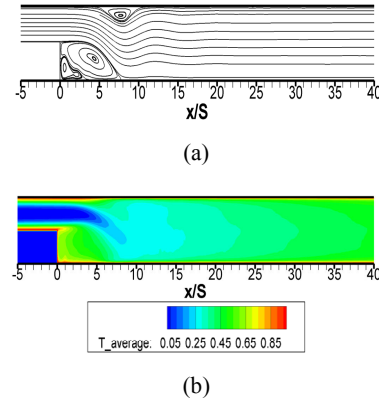

(a)

(b)

Fig. 5 (a) Streamlines and (b) temperature distribution of turbulent backward-facing step flows at Re=9000
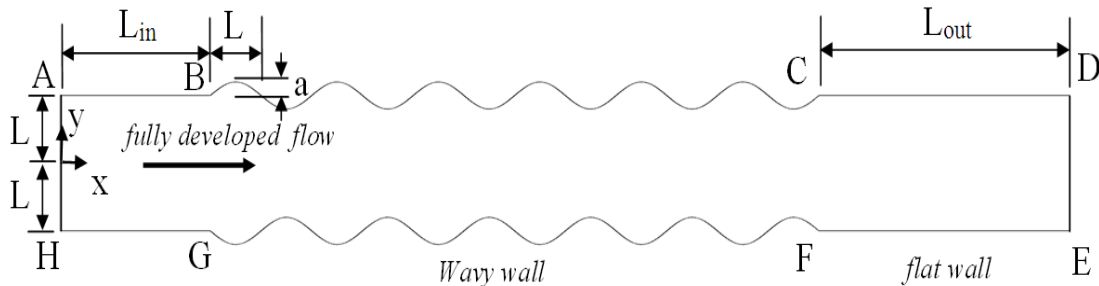
Fig. 6 Schematic view of the wavy channel flow

To estimate the heat transfer effect and the magnitude of drag in the wavy channel flow, the Nusselt number (Nu) and the skin-friction coefficient ($\operatorname{Re} C_f$) on the lower wavy boundary (G-F) are calculated. The local Nusselt number is defined as

$$Nu_x = h_x H / K_f = -\left(\frac{\partial T}{\partial n}\right) L / (T_w - T_{in}) \qquad (21)$$

where h_x and K_f are heat transfer coefficient and thermal conductivity respectively. The temperature gradient with respect to the orientation normal to the surface is calculated by

$$\frac{\partial T}{\partial n} = \sqrt{\left(\frac{\partial T}{\partial x}\right)^2 + \left(\frac{\partial T}{\partial y}\right)^2} \qquad (22)$$

The skin-friction coefficient is defined as $C_f = \tau_w / (\rho U_{in}^2)$. The shear stress on the surface given by

$$\tau_w = \mu \left(\frac{\partial u}{\partial y} + \frac{\partial v}{\partial x}\right)_{y=S(x)} \qquad (23)$$

Yields

$$\operatorname{Re} C_f = \frac{H}{U_{in}} \left(\frac{\partial u}{\partial y} + \frac{\partial v}{\partial x}\right)_{y=S(x)} \qquad (24)$$
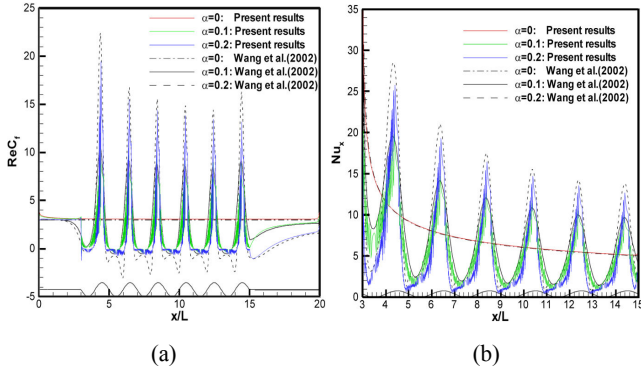
Fig. 7 is the distribution of skin-friction coefficients and Nusselt number in the laminar wavy channel flow of Pr= 6.93 at Re=500. The results present the same tendency with the results by Wang and Chen [20] except for the skin-friction coefficients at wave troughs in the cases of $\alpha = 0.2$. As fluid flowing into the wave troughs, the flow phenomena are restrained in the recirculation regions with low velocities. These would weaken the heat convection effects and give a negative skin-friction coefficient. On the contrary, fluids in the sections of wave crests are accelerated because of the narrowed passages in a symmetric wavy channel. Therefore, drag forces upwind the wave slopes are intensified and increase the skin-friction coefficients on the wave crests. These phenomena also contribute to the convective heat transfer effect of the wavy surface and give peaks of the Nusselt number on the crests. As shown in Fig. 7, the maximum skin-friction coefficient and Nusselt number occur on the first wave crest, which is the entrance of the wavy sections in the channel, and then decay

World Academy of Science, Engineering and Technology
International Journal of Aerospace and Mechanical Engineering
Vol:7, No:7, 2013

downstream. The case of $\alpha = 0$ represents the fluid flowing through a smooth channel in which the skin-friction coefficient and Nusselt number are decreased fast. Naturally, larger amplitude causes a greater influence on not only drag forces but also heat convection effects. In the case of $\alpha = 0.2$, a small vortex is formed behind the last wavy surface and also causes negative skin-friction coefficients.

(a)

(b)

Fig. 7 Distribution of (a) the skin-friction coefficients and (b) Nusselt number in the laminar wavy channel flow of Pr=6.93 at Re=500

In the simulation of turbulence, the Prandtl number is fiexd as Pr=1 with a subgrid Prandtl Number of 0.7. The average streamlines and isotherms of the turbulent wavy channel flow at Re=5000 are shown in Figs. 8 and 9. In the case of $\alpha = 0.1$, the structures of transient vortices at wavy troughs are the same as in laminar cases, and hence the tendency of skin-friction coefficient and Nusselt number are similar to those in the laminar cases except for the magnitude, as shown in Fig. 10. In turbulence, the heat convection effects are enhanced greatly by the fast and perturbed flow phenomena as well as the magnitude of drag force on the wavy surface. Although the Prandtl number in the turbulent cases is smaller than in laminar cases, the convection effects give larger and no-decayed Nusselt number on every wave crest, as sown in Fig. 10 (b).

As the amplitude increases to $\alpha = 0.2$, the vortices in the wave troughs are enlarged accompanying with small secondary ones formed near the surface. Fig. 10 indicates that these secondary vortices of the same velocity direction as flows upstream can cause the negative skin-friction coefficients at troughs changing into positive values inversely. Furthermore, the convection effects at the troughs are also improved. Fig. 11 is the distribution of skin-friction coefficient and Nusselt number for the turbulent case of $\alpha = 0.2$ at different Reynolds number. The results show the magnitude of drag and heat convection in turbulence of the wavy channel flow is reduced as Re decreases. Actually, the effects of the secondary vortices at troughs are weak in the case of Re=3000.
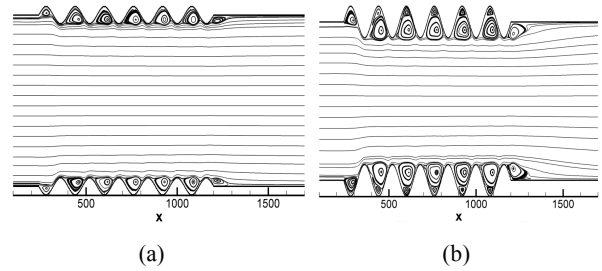

(a)

(b)

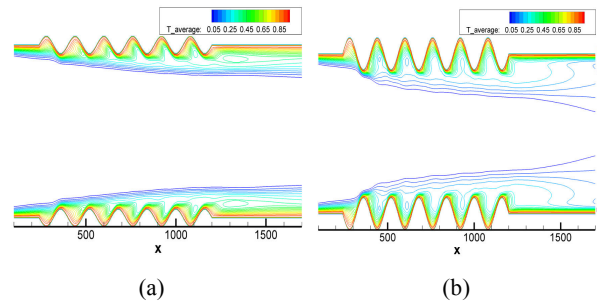Fig. 8 Turbulent streamlines of the wavy channel flow with (a) α=0.1 and (b) α=0.2 at Re=5000

(a)

(b)

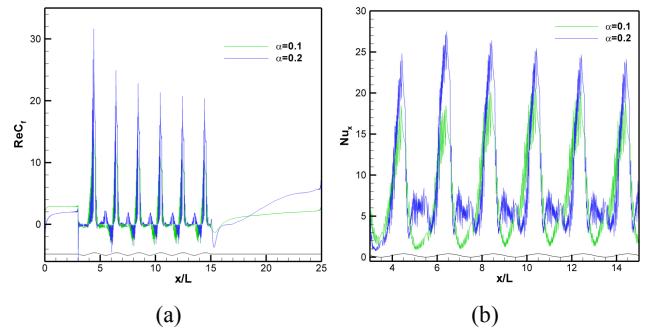Fig. 9 Turbulent isotherms of the wavy channel flow of Pr=1 with(a) α=0.1 and (b) α=0.2 at Re=5000

(a)

(b)

Fig. 10 Distribution of (a) the skin-friction coefficients and (b) Nusselt number in the turbulent wavy channel flow of Pr=1 at Re=5000
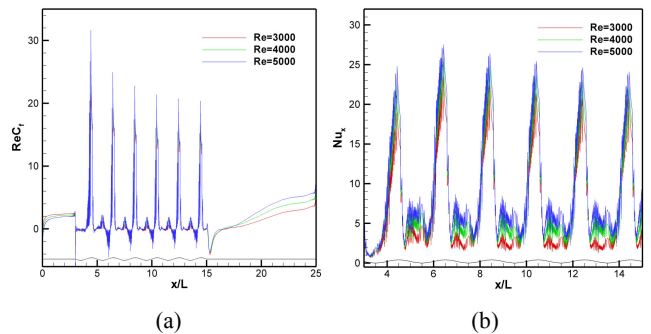

(a)

(b)

Fig. 11 Distribution of (a) the skin-friction coefficients and (b) Nusselt number in the turbulent wavy channel flow of Pr=1 with α=0.2 at different Reynolds number

REFERENCES

[1] G. R. McNamara and G. Zanetti, "Use of the Boltzmann equation to simulate lattice-gas automata," Phys. Rev. Lett., vol. 61, pp. 2332–2335, 1988.

[2] J. Zhang, "Lattice Boltzmann method for microfluidics: models and applications," Microfluid. Nanofluid., vol. 10, pp. 1–28, 2011.

[3] D. Grunau, S. Chen and K. Eggert, "A lattice Boltzmann model for multiphase fluid flows," Phys. Fluids, vol. 5, pp. 2557–2562, 1993.

[4] C. K. Chen, S. C. Chang, and S. Y. Sun, "Lattice Boltzmann method simulation of channel flow with square pillars inside by the field synergy principle," CMES-Comp. Model. Eng. Sci., vol. 22, pp. 203–215, 2007.

[5] Z. Guo and T. S. Zhao, "Lattice Boltzmann model for incompressible flows through porous media," Phys. Rev. E, vol. 66, p. 036304, 2002.

[6] S. C. Chang, Y. S. Hsu, and Chen CL, "Lattice Boltzmann simulation of fluid flows with fractal geometry: An unknown-index algorithm," J. Chin. Soc. Mech. Eng., vol. 32, pp. 523–531, 2011.

[7] P. L. Bhatnagar, E. P. Gross, and M. Krook, "A model for collision processes in gases. I. Small amplitude processes in charged and neutral one-component systems," Phys. Rev., vol. 94, pp. 511–521, 1954.

[8] S. Chen and GD Doolen, "Lattice Boltzmann model for fluid flows," Annu. Rev. Fluid Mech., vol. 30, pp. 329–364, 1998.

[9] H. Chen, S. Kandasamy, S. Orszag, R. Shock, S. Succi, and V. Yakhot, "Extended Boltzmann kinetic equation for turbulent flows," Science, vol. 301, pp. 633–636, 2003.

[10] J. W. Deardoff, "The use of subgrid transport equations in a three-dimensional model of atmospheric turbulence," J. Fluids Eng.-Trans. ASME, vol. 95, pp. 429–438, 1973.

[11] W. W. Kim, S. Menon, and H. C. Mongia, "Large eddy simulation of a gas turbine combustor flow," Combust. Sci. Technol., vol. 143, pp. 25–62, 1999.

[12] X. Zhou, K. H. Luo, and J. J. R. Williams, "Study of density effects in turbulent buoyant jets using large-eddy simulation," Theor. Comput. Fluid Dyn., vol. 15, pp. 95–120, 2001.

[13] G. Yu, E. J. Avital, and J. J. R. William, "Large eddy simulation of flow past free surface piercing circular cylinders," J. Fluids Eng.-Trans. ASME, vol. 130, p. 101304, 2008.

[14] S. M. Hashemian, M. Rahnama, and M. Farhadi, "Large eddy simulation of turbulent heat transfer in a channel with a square cylinder," Heat Transf. Eng., vol. 33, pp. 1052–1062, 2012.

[15] J. S. Smagorinsky, "General circulation experiments with the primitive equations— I. The basic experiment," Mon. Weather Rev., vol. 91, pp. 99–164, 1963.

[16] S. Hou, J. Sterling, S. Chen, and G. D. Doolen, "A lattice Boltzmann subgrid model for high Reynolds number flows," In *Pattern Formation and Lattice Gas Automata,* A. T. Lawniczak and R. Kapral, Ed. Fields Institute Communications American Mathematical Society, 1996, pp. 151–166.

[17] S. Chen, "A large-eddy-based lattice Boltzmann model for turbulent flow simulation," Appl. Math. Comput., vol. 215, pp. 591–598, 2009.

[18] H. Guan and C. Wu, "Large-eddy simulations of turbulent flows with lattice Boltzmann dynamics and dynamical system sub-grid models," Sci. China Ser. E-Technol. Sci., vol. 52, pp. 670–679, 2009.

[19] T. A. Rush, T. A. Newell, and A. M. Jacobi, "An experimental study of flow and heat transfer in sinusoidal wavy passages," Int. J. Heat Mass Transf., vol. 42, pp. 1541–1553, 1999.

[20] C. C. Wang and C. K. Chen, "Forced convection in a wavy-wall channel," Int. J. Heat Mass Transf., vol. 45, pp. 2587–2595, 2002.

[21] E. M. Alawadhi, "Forced convection flow in a wavy channel with a linearly increasing waviness at the entrance region," J. Heat Transf.-Trans. ASME, vol. 131, p. 011703, 2009.

[22] B. F. Armaly, F. Durst, J. C. F. Pereira, and B. T. Schonung, "Experimental and theoretical investigation of backward-facing step flow," J. Fluid Mech., vol. 127, pp. 473–496, 1983.

[23] E. Erturk, "Numerical solutions of 2-D steady incompressible flow over a backward-facing step. Part I: High Reynolds number solutions," Comput. Fluids, vol. 37, pp. 633–655, 2008.

[24] K. Ma, W. L. Wei, L. L. Wang, X. J. Zhao, "Large eddy numerical simulation of flows over a backward-facing step," International Symposium on Water Resource and Environmental Protection, vol. 4, pp. 3024–3026, 2011.

[25] L. Jongebloed, "Numerical study using FLUENT of the separation and reattachment points for backwards-facing step flow," Master's thesis in mechanical engineering, Rensselaer Polytechnic Institute, 2008.

[26] Y. H. Qian, D. d'Humiéres, P. Lallemand, "Lattice BGK models for Navier-Stokes equation," Europhys. Lett., vol. 17, pp. 479–484, 1992.

[27] X. Shan, "Simulation of Rayleigh-Bénard convection using a lattice Boltzmann method," Phys. Rev. E, vol. 55, pp. 2780–2788, 1997.

[28] X. Shan and H. Chen, "Lattice Boltzmann model for simulating flows with multiple phases and components," Phys. Rev. E, vol. 47, pp. 1815–1819, 1993.

[29] D. P. Ziegler, "Boundary conditions for lattice Boltzmann simulation," J. Stat. Phys., vol. 71, pp. 1171–1177, 1993.

Dr. Hsin-Yi Lai received his Ph.D. from the University of Wisconsin at Madison in 1984. He is currently working in National Cheng-Kung University as a full-time faculty member. Dr. Lai's research interests include engineering modeling of various micro-macro systems, design of experiments, and universe exploration. He had experiences in the application of modeling techniques for many different engineering systems. Dr. Lai is currently active in the professional societies of ASME, SME, ASEE and CSME.

Dr. Shing-Cheng Chang received his Ph.D. in Mechanical Engineering from National Cheng Kung University in Taiwan, 2010. He is a postdoctoral fellow of Department of Mechanical Engineering, National Cheng Kung University in Taiwan. His major research areas include computational fluid dynamics and nanotechnology. He has published 20 research papers in international journals, books, and conferences.